

## Articles

---

### Supramolecular Self-Assembly of *Escherichia coli* Glutamine Synthetase: Characterization of Dodecamer Stacking and High Order Association<sup>†</sup>

Joseph Yanchunas, Jr.,<sup>‡</sup> Michael J. Dabrowski,<sup>§</sup> Peter Schurke,<sup>§</sup> and William M. Atkins<sup>\*,§</sup>

Department of Medicinal Chemistry, School of Pharmacy, BG-20, University of Washington, Seattle, Washington 98195, and  
Macromolecular Structure Division, Bristol-Myers Squibb, Box 4000, Princeton, New Jersey 08543-4000

Received July 15, 1994; Revised Manuscript Received September 19, 1994<sup>⊗</sup>

**ABSTRACT:** Dodecameric glutamine synthetase (GS) from bacteria is formed from two face-to-face hexameric rings of identical subunits. These highly symmetrical aggregates from some bacteria, including *Escherichia coli*, "stack" in the presence of  $\text{Zn}^{2+}$  and other divalent ions to generate protein tubes (phase I) and subsequently associate side-to-side to yield "cables" and nonspecific aggregates (phase II). In order to understand the molecular mechanisms of recognition leading to this macromolecular self-assembly, the effects of solution conditions on the kinetics of these processes have been studied. These reactions have been monitored by changes in light scattering and by electron microscopy. Conditions have been established for isolation of phases I and II. At 0.04 mg of GS/mL, pH 7.0, 100 mM KCl, and 1 mM  $\text{Mn}^{2+}$ , 25 °C, minimal side-to-side aggregation occurs, and the stacking reaction follows second-order kinetics, with respect to GS, at low extent of reaction. The second-order rate constants determined for phase I, initiated by  $\text{Zn}^{2+}$  or  $\text{Co}^{2+}$ , demonstrate a pH optimum at 7.0–7.25, whereas phase II is favored at pHs below 6.5. The pH profile for the stacking reaction suggests that His residues are involved, and modification of 2–3 histidines/subunit with diethyl pyrocarbonate (DEPC) is sufficient to completely inhibit metal-dependent dodecamer stacking. The effect of ionic strength on GS stacking was also studied. Although hydrophobic interactions have previously been assumed to dominate this protein–protein association, both phase I and phase II of the assembly are inhibited by KCl and NaCl, suggesting that ionic interactions also play an essential role. Lastly, the metal ion specificity for the phase I reaction was determined. Although  $\text{Zn}^{2+}$ - and  $\text{Co}^{2+}$ -mediated GS stacking has been studied most extensively,  $\text{Cu}^{2+}$  is a more potent initiator of tubule assembly. The concentration of  $\text{Cu}^{2+}$  required for half-maximal rates of stacking ( $C_{1/2}$ ) is 80  $\mu\text{M}$ . Of the metal ions examined, the order of the efficacy for supporting GS stacking is  $\text{Cu}^{2+} > \text{Zn}^{2+}$ ,  $\text{Hg}^{2+} > \text{Cd}^{2+} \gg \text{Ni}^{2+}$ ,  $\text{Co}^{2+}$ . The divalent ions  $\text{Fe}^{2+}$  and  $\text{Ca}^{2+}$  do not support GS stacking. These studies indicate that phases I and II of GS association can be controlled through manipulation of the solution conditions.

Protein–protein interactions are necessary for many aspects of metabolic regulation and structural maintenance

of cellular constituents *in vivo*. Interest in the mechanisms of protein–protein recognition is no longer limited, however, to physiological processes. The inherent molecular recognition found in supramolecular protein assemblies recently has been appreciated as a potential guide for the design and *in vitro* production of biomaterials with useful structural, catalytic, and regulatory properties (Whitesides et al., 1992; McGrath et al., 1992; Bhatia et al., 1992; Grove et al., 1993;

<sup>†</sup> This work was supported by the Whitaker Foundation (93-0272).

<sup>\*</sup> Corresponding author [telephone (206) 685-0379; FAX (206) 685-3252].

<sup>‡</sup> Bristol-Myers Squibb.

<sup>§</sup> University of Washington.

<sup>⊗</sup> Abstract published in *Advance ACS Abstracts*, November 15, 1994.

Jorgensen, 1993). In particular, the utility of self-assembling protein arrays as biomineralization templates, as ordered polymeric supports in molecular devices and in the production of nanostructures, seems limitless (Ozin, 1992; Gleiter, 1992). At this early stage in the development of protein engineering as a source of biomaterials, it is essential to identify proteins with properties that may be useful in the construction of patterned macromolecular assemblies, and it is necessary to characterize proteins that display novel macromolecular recognition.

A dramatic example of a supramolecular protein assembly is the highly symmetric dodecameric bacterial glutamine synthetase (GS).<sup>1</sup> GS plays a critical role in nitrogen metabolism of bacteria, catalyzing the ATP-dependent conversion of glutamate to glutamine. GS is catalytically functional with either two  $Mg^{2+}$  or two  $Mn^{2+}$  ions bound at each of the active sites. Some bacterial GSs are regulated by covalent adenylation, which results in inactivation of the  $Mg^{2+}$ -GS. Two decades ago, electron microscopy experiments demonstrated that the *Escherichia coli* glutamine synthetase dodecamer of identical subunits is formed from two hexagonal rings stacked face to face (Valentine et al., 1968). The X-ray crystal structure of the unadenylylated *Salmonella typhimurium* enzyme more recently has provided a molecular model of the specific interactions required to maintain this symmetric, dodecameric structure in the absence of substrates and in the presence of several ligands (Almassy et al., 1986; Liaw & Eisenberg, 1994; Liaw et al., 1993). No crystal structure is available for the adenylylated enzyme.

After it was demonstrated that GS is a complex oligomer with hexameric ring structure, it was observed that individual GS molecules from several bacteria self-assemble into stacked fibers, or "tubes" of dodecamers, in the presence of  $Zn^{2+}$  or  $Co^{2+}$  (Miller et al., 1974). These aggregates eventually precipitate from solution. Electron microscopy and optical image analysis of samples containing the  $Co^{2+}$ -precipitated form of *E. coli* GS have indicated that these highly ordered fibers wind into three- and seven-stranded protein cables at low temperatures (Frey et al., 1975). The metal-induced aggregation has been exploited to aid in the purification of some GS enzymes, including the isozymes from *E. coli*, *S. typhimurium*, and *Pseudomonas putida* (Miller et al., 1974). However, other dodecameric bacterial GS enzymes do not precipitate in the presence of  $Zn^{2+}$  or  $Co^{2+}$ . In addition, octameric mammalian GS does not self-assemble into aggregates in the presence of these divalent cations (Denman & Wedler, 1984), and thermally induced aggregation of some dodecameric GS enzymes leads to formation of nonspecific aggregates which lack periodic structure (Merkler et al., 1988). Thus, the protein tubes formed by some GS enzymes apparently result from specific metal-dependent interactions between individual dodecamers. Since the discovery of this macromolecular self-association, few data have addressed the mechanism of this reaction, and the physiological role of this assembly remains unknown. Current interest in design of self-organizing protein arrays (McGrath et al., 1992) and in design of metal-dependent

protein assemblies (Ghadiri et al., 1992) prompted us to consider the potential utility of *E. coli* GS as a raw material with useful self-assembly properties. In addition to the inherent feature of metal-directed self-assembly, GS possesses other characteristics which make it a potentially useful biomaterial. The protein is remarkably robust and retains its gross structural properties at elevated temperatures (Shrake et al., 1989), at elevated pressures (Atkins, 1994, accompanying paper), and in solutions containing organic solvent (see Materials and Methods). Furthermore, the gene encoding the *E. coli* GS has been cloned and overexpressed (Colombo & Villafranca, 1986), allowing for genetic manipulation and production of large quantities of structural variants.

In order to understand the molecular mechanisms of this macromolecular assembly, a fundamental characterization of this reaction under a variety of conditions is necessary. Structural studies have been performed with  $Co^{2+}$ -induced GS aggregates (Frey et al., 1975), and the kinetics of  $Zn^{2+}$ -induced formation of GS tubes have been examined (Maurizi et al., 1986). However, a systematic characterization of this reaction with purified GS preparations that are homogeneous with respect to adenylation state has not been previously reported. The previous studies have been performed under different conditions with GS preparations of varying adenylation state, and no explanation for the differences in structures observed by electron microscopy in individual experiments has been proposed. In this series of papers, we examine the solution conditions affecting the assembly reaction, determine the kinetic parameters for GS "stacking", and present evidence for a molecular mechanism of this macromolecular recognition, including identification of the metal ligands involved.

## MATERIALS AND METHODS

**Protein Purification.** Purified GS was obtained by previously described methods, utilizing the  $Zn^{2+}$ -precipitation step (Miller et al., 1974). Briefly, streptomycin sulfate is added to crude *E. coli* cell supernatant, and the supernatant following centrifugation is made 2 mM  $Zn^{2+}$ . The pellet following centrifugation is resuspended by extensive dialysis against 20 mM imidazole, pH 7.2, 10 mM EDTA, and 10 mM  $MgCl_2$  and then against 50 mM imidazole, pH 7.2, 1 mM  $MnCl_2$ , and 100 mM KCl. The resulting solution is titrated to pH 5.8 by addition of acetic acid, and acetone is added dropwise to a final concentration of 45% (v/v). The pellet following centrifugation is resuspended in 50 mM Hepes, pH 7.2, 10 mM  $MnCl_2$ , and 100 mM KCl. Notably, the acetone precipitation step has yielded fully active GS regardless of the temperature (4 vs 25 °C) of samples throughout exposure to acetone. The resuspended pellet, resulting from acetone precipitation, is made 10% ammonium sulfate [v/v, from saturated  $(NH_4)_2SO_4$ ] and brought to pH 4.5 by addition of 0.1 M acetic acid. Completely unadenylylated enzyme preparations were obtained from bacterial expression systems utilizing a cloned GS in *E. coli* strain YMC21E. This strain lacks a chromosomal GS gene. In addition, the *Atase* gene has been deleted from YMC21E (Chen et al., 1982). The protein preparations obtained from this strain are completely unadenylylated ( $n = 0$ ), based on the  $\gamma$ -glutamyl transferase assay (Woolfolk et al., 1974; Stadtman et al., 1979). Typically, a 10-L fermentation yields 200–300 mg of purified protein.

<sup>1</sup> Abbreviations: GS, glutamine synthetase; Hepes, 4-(2-hydroxyethyl)piperazineethanesulfonic acid; ATP, adenosine 5'-triphosphate; keV, kiloelectronvolts; EDTA, ethylenediaminetetraacetic acid; MSOX, methionine sulfoximine; DEPC, diethyl pyrocarbonate.

**Assay for Supramolecular Assembly.** Light scattering measurements provide one assay for the self-assembly reaction. The measurements were performed on an SLM-Aminco 8000C fluorometer in the analog detection mode. Excitation and emission wavelengths were 340 nm. Slit widths were 4 mm, and the integration time was 0.2 s. The sample holder was thermostated with a circulating water bath, and samples were stirred throughout the measurements. After a stable baseline was obtained with samples of varying composition in a volume of 2 mL,  $\text{ZnSO}_4$  or another metal salt was added at a final concentration indicated in the figures. It was observed that  $\text{Cu}^{2+}$  caused an increase in the background intensity of scattered light, in the absence of protein. The increase in intensity was approximately 10% of the total change in intensity when GS was included. Therefore, a time-dependent baseline obtained after addition of  $\text{Cu}^{2+}$  in the absence of GS was subtracted from the light scattering measurement in the presence of GS.

**Kinetic Analysis.** At 0.04 mg of protein/mL (0.063  $\mu\text{M}$  dodecamers), 200  $\mu\text{M}$   $\text{Zn}^{2+}$ , and 100 mM KCl, pH 7.0, 20 °C, the initial stacking phase (phase I) was sufficiently isolated from side-to-side interactions to allow for analysis of the initial rates of this reaction. The analysis of GS stacking kinetics by light scattering assumes that  $[(I_t - I_0)/(I_\infty - I_0)][\text{GS}]_0$  is the concentration of GS that is in stacked complexes, where  $I_0$ ,  $I_t$ ,  $I_\infty$ , and  $[\text{GS}]_0$  are the light scattering intensities before addition of metal, at time  $t$  after addition of metal, and at the plateau intensity ( $t = \infty$ ) and  $[\text{GS}]_0$  is the total concentration of GS dodecamers, respectively. Second-order rate constants were determined from nonlinear regression analysis of light scattering intensity vs time, using eq 1, where  $k$  is the second-order rate constant. Integration and substitution into (1) yields eq 2. All second-order kinetic

$$kt = 1/[\text{GS}]_t - 1/[\text{GS}]_0 \quad (1)$$

$$I_t = (I_0 + I_\infty[\text{GS}]_0 kt)/([\text{GS}]_0 kt + 1) \quad (2)$$

analyses included light scattering data that spanned at least 2 half-lives. Because light scattering intensity disproportionately will reflect larger aggregates in heterogeneous mixtures, this analysis does not measure the kinetics of the reaction  $\text{GS}_n + \text{GS} = \text{GS}_{n+1}$ . Instead, this analysis yields an approximate second-order rate constant for two individual dodecamers forming a complex. Therefore, the analysis is limited to low extent of reaction. The analysis assumes that, although heterogeneity in molecular species is expected, the  $I_\infty$  values represent the weighted average of the molecular weight of species present at completion of the reaction and that this value is not altered with the conditions changed within a given experiment. The data support this assumption. Light scattering values for  $t = \infty$  were considered acceptable when the scattered intensity did not change by more than 5% over 30 min. Nonlinear regression was performed with the software Enzfitter by Biosoft.

**Electron Microscopy.** Transmission electron microscopy was performed on a JEOL electron microscope, with an acceleration potential of 80 keV. Samples were prepared by placing a drop of protein solution on a Formvar-coated copper grid (200 mesh, Fullam, Inc., Latham, NY). After 3 min the solution was blotted and air-dried. A drop of 2% (w/v) uranyl acetate was added. After 4 min the negatively

stained samples were blotted and allowed to air-dry. Samples were prepared immediately prior to microscopy. All electron micrographs were obtained at 60000 $\times$  magnification. The EM micrographs in Figure 1 are at 240000–250000 $\times$  magnification.

**Chemical Modification.** Purified GS (21  $\mu\text{M}$  subunits) in 1 mL of 40 mM Hepes, pH 7.0, and 10 mM  $\text{MgCl}_2$  at 25 °C was modified with DEPC by addition of a stock solution in ethanol. The concentration of reactive DEPC in stock solutions was determined immediately prior to use by the method of Miles (1977). The final concentration of DEPC in GS-samples varied from 0 to 250  $\mu\text{M}$ . The extent of modification of GS was determined spectrophotometrically (278 nm,  $\epsilon = 1310 \text{ M}^{-1} \text{ cm}^{-1}$ ; Miles, 1977). The modified GS samples were then dialyzed against 50 mM Hepes, pH 7.0, 100 mM KCl, and 1 mM  $\text{MnCl}_2$  to remove excess DEPC.

Inactivation of GS with MSOX and ATP was accomplished by addition of 5 mM MSOX and 5 mM ATP to purified GS (70  $\mu\text{M}$  subunits) in 50 mM Hepes, pH 7.0, 100 mM KCl, and 1 mM  $\text{MnCl}_2$ . After 30 min, samples were dialyzed to remove excess MSOX and ATP.  $\gamma$ -Glutamyl transferase assays (Woolfolk et al., 1966) demonstrated that these GS samples were completely inactivated, and the amount of ADP bound was spectrophotometrically estimated to be 10–11 ADP/dodecamer.

## RESULTS

**Definition of the Reactions.** Previous results have indicated that the  $\text{Zn}^{2+}$ - or  $\text{Co}^{2+}$ -induced aggregation of *E. coli* GS is complex, consisting of several molecular interactions and distinct phases of aggregation including face-to-face stacking of individual dodecamers to form tubes (phase I), side-to-side annealing of these tubes to form "ropes", and eventual formation of complex "wheat-sheaf" structures with bundles of these ropes (phase II; Valentine et al., 1968). Furthermore, nonspecific side-to-side reactions may occur simultaneously, yielding complex, disordered aggregates. The contribution of each of these phases of aggregation is extremely sensitive to the solution conditions used. In order to study the phase I stacking reaction, we sought conditions which allowed for minimal side-to-side aggregation of stacked complexes.

Light scattering can be used as a faithful measure of the phase I reaction of  $\text{Mn}^{2+}$ -GS when the total protein concentration is kept below 0.05 mg/mL, the temperature is kept at or below 25 °C, and the pH is 6.8–8.0. If these conditions are not maintained, then significant side-to-side aggregation of the stacked complexes occurs and this contributes to the changes in light scattering intensity. Typical light scattering curves obtained with  $\text{Zn}^{2+}$ -induced aggregation of GS under different conditions are shown in Figure 1. The EM micrographs for samples removed at various times demonstrate that the average length of GS tubes increases with time after addition of  $\text{Zn}^{2+}$ , as seen previously with MSOX-ATP-inactivated GS (Maurizi et al., 1986). The results indicate that addition of metal is required to initiate the reaction and that side-to-side association of the initially formed tubes occurs relatively late in the reaction. Addition of 5 mM EDTA at any point in the progress curve results in rapid return of the scattered light intensity to initial levels, and stacked dodecamers are not evident in EM

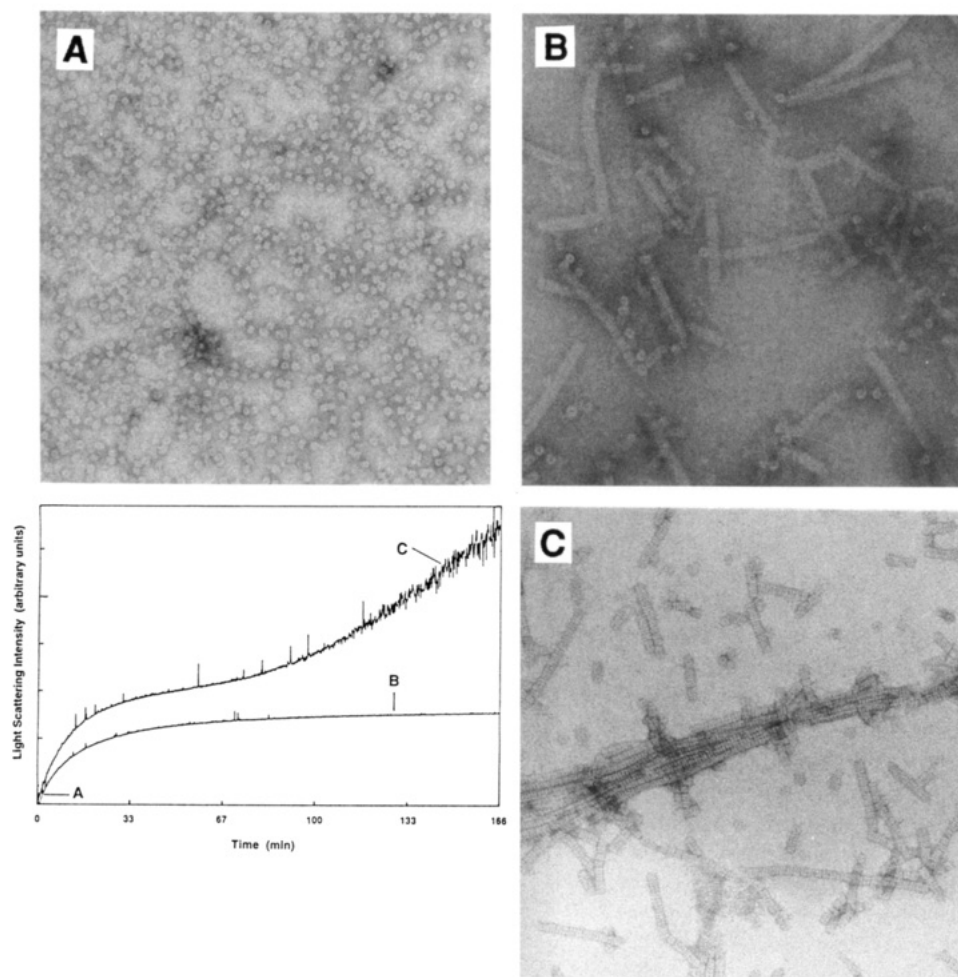


FIGURE 1: Light scattering changes after addition of  $\text{Zn}^{2+}$  to dodecameric GS.  $\text{Zn}^{2+}$  was added at time = 0 to a solution containing either 0.02 mg of GS/mL, pH 7.2, 1 mM  $\text{MnCl}_2$ , and 100 mM KCl, 25 °C (bottom curve, A and B), or 0.08 mg of GS/mL, pH 6.8, 1 mM  $\text{MnCl}_2$ , and 100 mM KCl, 25 °C (top curve, C). Samples were removed from either reaction at the indicated times and examined by electron microscopy, panels A–C (magnification is approximately 240000 $\times$ ; reproduced at 75% of original size). The second rise in light scattering intensity, sample C, corresponds to side-to-side aggregation of stacked GS tubes.

micrographs, as observed by others (Maurizi et al., 1986; data not shown). As expected, at later time points there is increased side-to-side and higher order aggregation when conditions allow (phase II). Therefore, we propose that the second rise in light scattering intensity, which occurs in samples at high protein concentration and low pH (Figure 1C), results from several types of side-to-side interactions of initially formed GS tubes. We have not attempted to determine specifically the kinetics of side-to-side aggregation of stacked tubes. The progress curves and the EM micrographs shown in Figure 1 demonstrate that the extent of phase II can be minimized at low protein concentrations and near pH 7.5. Presumably, the tendency for stacked complexes to aggregate side to side is a function of their length, and at low protein concentrations the average length of stacked tubes is minimized. Other solution conditions affect the extent of side-to-side aggregation as well. Specifically, lowering the pH below 6.8, increasing the protein concentration, and decreasing the salt concentration result in more extensive side-to-side aggregation (data not shown). The temperature and pressure dependence of GS stacking is examined in detail in an accompanying paper. We also observed that, at high concentrations of metal ions, phase I and phase II cannot be temporally separated. Under conditions which allow for separation of these phases at 200  $\mu\text{M}$   $\text{Zn}^{2+}$ , increasing the  $\text{Zn}^{2+}$  concentration to >500  $\mu\text{M}$  leads

to a second rise in light scattering intensity before phase I has reached a stable plateau. One possible reason for this is that phase II may be dependent on metal ions as well. This possibility is discussed, along with the experiments which compare metal ion specificity, below.

Having established a range of conditions which provide negligible side-to-side aggregation of stacked GS, it is possible to quantitatively determine the effect of solution conditions on the phase I stacking reaction. First, it was essential to generate a useful kinetic model to quantitate the observed rates of stacking. Others have demonstrated that the self-assembly kinetics of GS stacking fit well to a bimolecular kinetic model (Maurizi et al., 1986) when fluorescence changes of extrinsically labeled GS are used to monitor GS stacking. We have applied this simplifying model to the results obtained with light scattering experiments. Results of experiments performed at two GS concentrations are shown in Figure 2, in which values for light scattering intensity are fit directly to the bimolecular rate equation by nonlinear regression. These results show that the kinetics of phase I determined by light scattering measurements closely approximate a simple bimolecular reaction at low extent of reaction, as previously documented with fluorescence methods (Maurizi et al., 1986). The rate constants,  $k$ , recovered in experiments with different concentrations of GS are in excellent agreement with each other

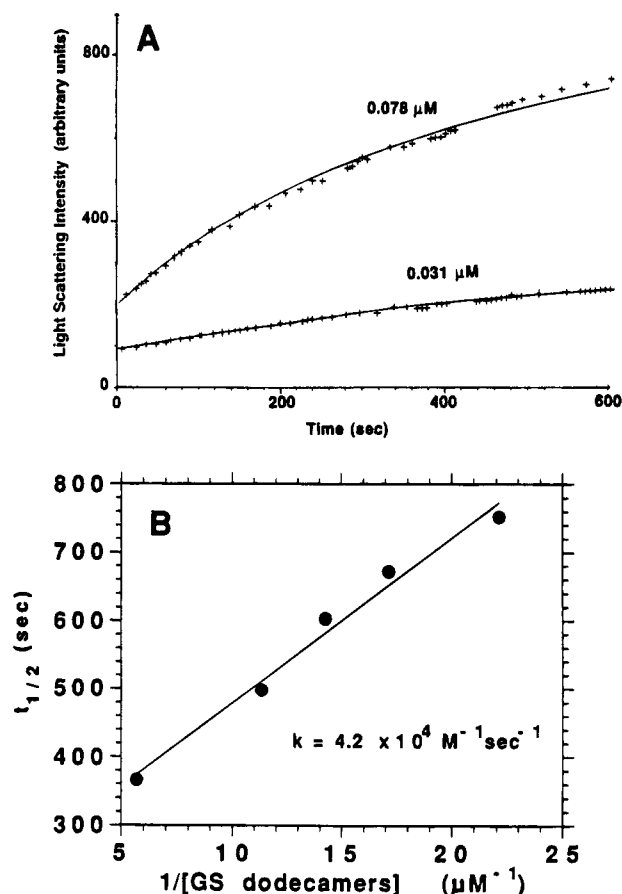


FIGURE 2: (A) Nonlinear regression of light scattering data obtained at two GS concentrations (0.078 and 0.031  $\mu\text{M}$ ). The data for the first 10 min of the reaction are fit to a bimolecular rate equation (solid lines). Samples were at pH 7.0 with 1 mM  $\text{MnCl}_2$  and 100 mM KCl at 20  $^\circ\text{C}$  with the indicated concentrations of GS subunits. (B) Dependence of apparent half-lives for disappearance of free GS dodecamers on protein concentration. The half-lives for complete stacking of GS at several concentrations are plotted vs  $1/[\text{free GS dodecamers}]$ . The second-order rate constant obtained from this analysis is  $4.2 \times 10^4 \text{ M}^{-1} \text{ s}^{-1}$ .

and with the rate constants previously determined under different conditions (Maurizi et al., 1986). The rate constants recovered from the results shown in Figure 2 are  $3.1 \times 10^4 \text{ M}^{-1} \text{ s}^{-1}$  and  $1.4 \times 10^4 \text{ M}^{-1} \text{ s}^{-1}$  for the samples containing 0.078 and 0.031  $\mu\text{M}$  GS, respectively. The reduced  $\chi^2$  values for the nonlinear regression shown in Figure 2A are 2.18 and 6.2 for concentrations of 0.031 and 0.078  $\mu\text{M}$  GS subunits, respectively. When the last few data points (500–600 s) are excluded from the analysis, the  $\chi^2$  value for the 0.078  $\mu\text{M}$  GS experiment decreases to 3.1. We observed that as the protein concentration is increased, the bimolecular model fits less well to the data, and the recovered fits overestimate the apparent rate of reaction. We propose that, at higher concentrations of GS, side-to-side reactions occur earlier in the progress curve and contribute to the increase in light scattering intensity. Hence, we have limited the bimolecular rate analysis to experiments where the protein concentration is kept below 0.05 mg/mL (0.078  $\mu\text{M}$  subunits). It is essential to note that at temperatures above 25  $^\circ\text{C}$  (data not shown) and at protein concentrations above 0.05 mg/mL (Figure 1) the kinetics of the reaction deviate significantly from this model. The data provided here indicate that the reason for this deviation is that side-to-side aggregation contributes to the observed light scattering intensity when conditions are not carefully controlled.

**Effect of Concentration on Half-Life.** In order to verify that bimolecular reaction kinetics apply to phase I (with respect to GS), the concentration dependence of the half-lives for disappearance of free dodecamers was determined in the presence of 100 mM KCl and 1 mM  $\text{MnCl}_2$ , pH 7.0 at 25  $^\circ\text{C}$ . The half-lives for the disappearance of free GS dodecamers were determined empirically, without fitting the data to a bimolecular kinetic model, and plotted vs  $1/[\text{GS}]_0$ . If the reaction kinetics are described by a bimolecular rate law, then the reaction half-life  $t_{1/2} = 1/k[\text{GS}]_0$ . A plot of  $t_1$  vs  $1/[\text{GS}]_0$  yields a line with a slope corresponding to a  $k_1$  value of  $4.2 \times 10^4 \text{ M}^{-1} \text{ s}^{-1}$  at 25  $^\circ\text{C}$  ( $r^2 = 0.998$ ). This value is in excellent agreement with the rate constants obtained by fitting the data to the bimolecular model. The linear dependence of the reaction half-life on concentration provides additional support for the bimolecular reaction kinetics.

**Effect of pH.** The bimolecular rate constants of phase I stacking were determined at several pHs, in a series of buffers maintained at constant ionic strength by addition of KCl. Each of these buffers had ionic strength equivalent to that of the 50 mM Hepes, 100 mM KCl, and 1 mM  $\text{MnCl}_2$  used as the standard buffer in other assays. The  $\text{Zn}^{2+}$ -induced stacking reaction exhibits a maximum rate at pH 7.25, and there is an apparent  $\text{pK}_a$  of 6.9–7.0 for this reaction. At 25  $^\circ\text{C}$  the second-order rate constants range from  $(0.7 \pm 0.05) \times 10^4 \text{ M}^{-1} \text{ s}^{-1}$  at pH 6.5 to  $(1.35 \pm 0.06) \times 10^4 \text{ M}^{-1} \text{ s}^{-1}$  at pH 7.25. Because it is possible that the different metal ions which induce GS stacking have different binding sites, we have also analyzed the pH profile of the  $\text{Co}^{2+}$ -mediated reaction. A nearly identical result is obtained with the  $\text{Co}^{2+}$ -induced reaction (1 mM  $\text{Co}^{2+}$ ). These results are summarized in Figure 3.

A striking difference is observed when the  $\text{Zn}^{2+}$ -dependent phase II reactions are examined. The higher order aggregation is markedly favored at the lower pHs. In fact, at the more basic pHs, the second arm of the light scattering trace is nearly abolished. Whereas phase I demonstrates a 2-fold increase in rate when the pH is raised from pH 6.5 to pH 7.5, phase II is inhibited by approximately 15-fold over the same pH range (Figure 3). Apparently the different phases of the reaction are controlled by different ionization reactions. For  $\text{Co}^{2+}$ -mediated aggregation, phase II is even more dramatically enhanced as the pH is lowered (not shown).

**Effect of Histidine Modification.** The pH dependence of the phase I stacking reaction suggests that histidines play a role in binding the metal ion. Moreover, essentially all  $\text{Zn}^{2+}$  binding proteins either have glutamate/aspartate or histidine/cysteine combinations of metal ligands (O'Halloran, 1993; Karlin, 1993). For these reasons, we have performed chemical modification studies with the histidine-specific reagent diethyl pyrocarbonate (DEPC). This reagent demonstrates specificity for histidine modification and provides a spectroscopic probe of the extent of modification (Miles, 1977). First, substrate-free GS was treated with 200  $\mu\text{M}$  DEPC, and the modification of histidine residues was monitored spectrophotometrically (Miles, 1977). After modification of an average of 1 histidine/subunit, the relative rate of  $\text{Zn}^{2+}$ -induced stacking is reduced to 46% of untreated samples. Complete inhibition of GS stacking is obtained after modification of 3 histidines/subunit (Table 1). The X-ray crystal structure of the substrate-free *S. typhimurium* GS indicates that, of the 16 histidines contained in the E.

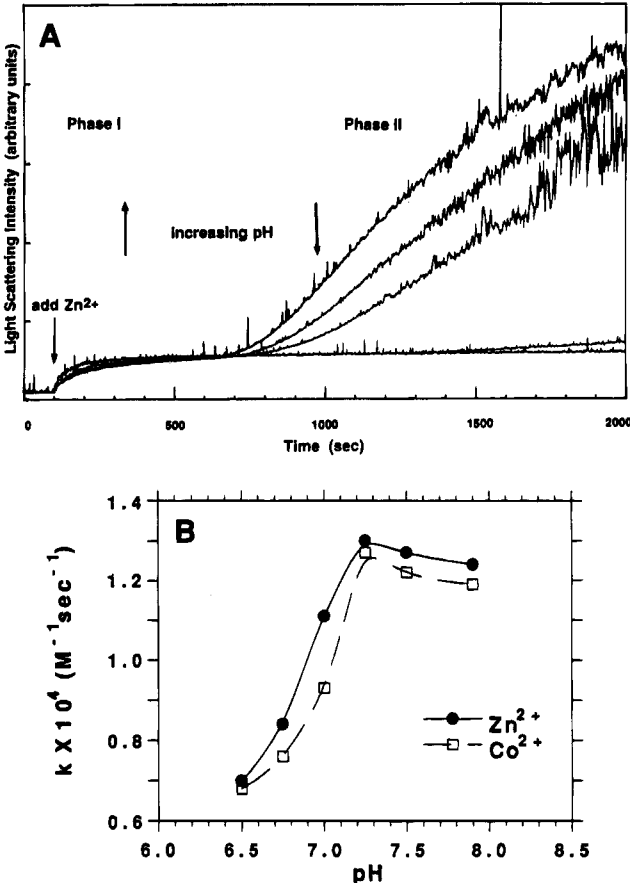


FIGURE 3: (A) Effect of pH on phase I and phase II of  $\text{Zn}^{2+}$ -induced GS aggregation. Light scattering changes after addition of  $100 \mu\text{M}$   $\text{Zn}^{2+}$  to samples containing  $0.1 \text{ mg}$  of GS/mL,  $1 \text{ mM}$   $\text{MnCl}_2$ , and  $100 \text{ mM}$  KCl at pH 6.5, 6.8, 7.0, 7.25, and 7.5 are shown. Reaction rates of phase I increase with increasing pH, whereas rates of phase II decrease. (B) Bimolecular rate constant for GS stacking, phase I, at several pHs. Samples contained  $0.04 \text{ mg}$  of GS/mL,  $1 \text{ mM}$   $\text{MnCl}_2$ , and either  $100 \mu\text{M}$   $\text{Zn}^{2+}$  or  $1 \text{ mM}$   $\text{Co}^{2+}$ . The ionic strength was held constant by addition of KCl after the desired pH was obtained.

Table 1: Effect of Histidine Modification on GS Stacking<sup>a</sup>

no. of His modified/dodecamer	second-order rate constant ( $\text{M}^{-1} \text{ s}^{-1}$ )
0	$1.3 \times 10^4$
1.1	$5.9 \times 10^3$
1.9	$2.1 \times 10^2$
2.8	$<1 \times 10^1$

<sup>a</sup> The average number of histidines modified per dodecamer is determined from the  $\epsilon^{230}$  according to Miles (1977). Rate constants were determined at  $293^\circ\text{C}$ , with samples containing  $0.05 \text{ mg}$  of GS/mL,  $50 \text{ mM}$  Hepes, pH 7.0,  $1 \text{ mM}$   $\text{MnCl}_2$ , and  $100 \text{ mM}$  KCl.

*coli* protein, 1 is present in the active site (His-269) and provides a metal ligand to a catalytic  $\text{Mn}^{2+}$  ion. His-271 also lies within the active site. Three other histidines are far from the active site and are fully exposed to solvent. In the absence of substrates, it is possible that the active site histidines are subject to modification by DEPC. Therefore, a second set of chemical modification experiments was performed. GS samples were first inactivated with ATP and methionine sulfoximine (MSOX). This treatment is known to result in inhibition of GS by forming a metal-ligated (methionine sulfoximine phosphate)-ADP complex at the active site, which can only be removed by acid treatment (Rowe et al., 1969; Maurizi & Ginsburg, 1982). The

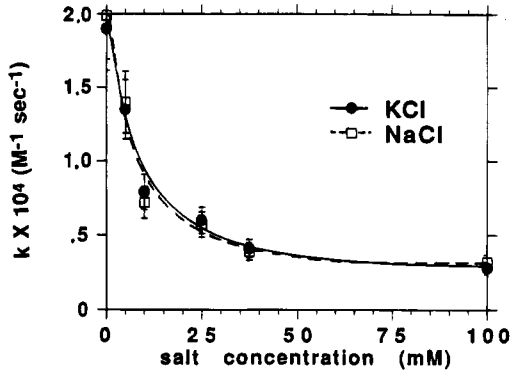


FIGURE 4: Effect of salt concentration on phase I of  $\text{Zn}^{2+}$ -induced stacking. Bimolecular rate constants for phase I are shown at several concentrations of KCl and NaCl. Samples contained  $0.04 \text{ mg}$  of GS/mL,  $50 \text{ mM}$  Hepes, pH 7.0, and  $1 \text{ mM}$   $\text{MnCl}_2$ , at  $25^\circ\text{C}$ .

MSOX-ATP inactivation was done in order to protect the active site histidine(s) from modification with DEPC. The ATP-MSOX-inactivated enzyme demonstrates "normal" stacking behavior in the presence of  $\text{Zn}^{2+}$  (not shown); however, modification of approximately 2 histidines with DEPC is sufficient to completely inhibit this self-assembly reaction even in the MSOX-inactivated GS. Together with the results obtained with active GS, this suggests that the active site histidines do not play a crucial role in GS stacking. The role of specific histidines in the stacking reaction is examined in more detail in a subsequent paper in this series (Dabrowski et al., 1994).

**Effect of Salt Concentration.** The effects of ionic strength on the phase I reaction, at a single temperature and pH, were also studied. The reference conditions described above were used except no KCl was included in the buffer. Several reactions were then initiated in the presence of varying concentrations of KCl. The results are summarized in Figure 4. It is clear that  $10 \text{ mM}$  KCl is sufficient to decrease the rate of the stacking reaction by 60%. Similar results are obtained when NaCl is used to replace KCl, suggesting that the effect is due to ionic strength, rather than a molecular interaction requiring specific ions. These results suggest that the stacking reaction is dependent on some ionic interaction between stacked dodecamers.

We have also performed experiments under conditions in which the phase II reactions are observed. The phase II reactions are dramatically inhibited by KCl and NaCl, suggesting that they also involve ionic interactions between stacked complexes (data not shown).

**Metal Ion Specificity.** The metal ion specificity for the stacking reaction was also examined. Previously published results suggest that divalent metal ions other than  $\text{Zn}^{2+}$  and  $\text{Co}^{2+}$  do not result in precipitation of *E. coli* GS from crude cell extracts. In particular,  $\text{Cu}^{2+}$  and  $\text{Hg}^{2+}$  were suggested to result in incomplete precipitation of GS from cell extracts, and  $\text{Zn}^{2+}$  was found to be the most selective and potent ion for this purpose (Miller et al., 1974). However, a direct comparison of the relative affinities of these metal ions with purified preparations has not been previously reported. Therefore, we have determined the relative bimolecular rate constants for GS stacking initiated by several divalent metal ions. This has been done in the presence of  $100 \text{ mM}$  KCl, in order to minimize nonspecific salt effects from the metal ions, as described above. Indeed, this comparison reveals that  $\text{Zn}^{2+}$  is not the most potent metal ion in supporting GS



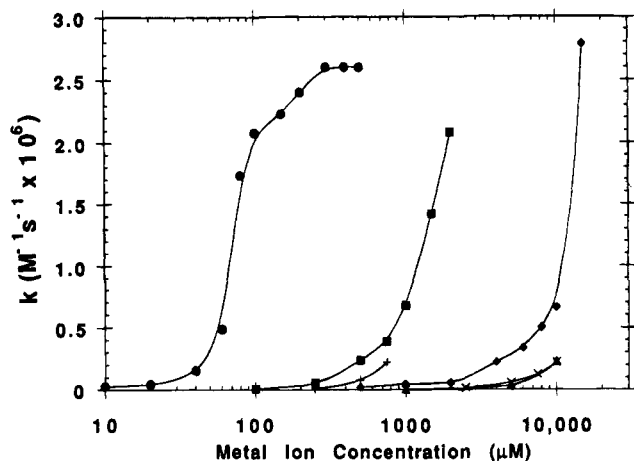


FIGURE 5: Relative efficacy of divalent metal ions in initiating GS stacking. The rate constants for GS stacking are plotted vs the total metal ion concentration for  $\text{Cu}^{2+}$  (closed circles),  $\text{Hg}^{2+}$  (crosses),  $\text{Zn}^{2+}$  (closed squares),  $\text{Cd}^{2+}$  (closed diamonds),  $\text{Ni}^{2+}$  (closed triangles), and  $\text{Co}^{2+}$  ( $\times$ 's). No stacking is observed in the absence of these ions. Samples contained  $0.031 \mu\text{M}$  GS subunits,  $50 \text{ mM}$  Hepes,  $\text{pH } 7.0$ ,  $100 \text{ mM}$  KCl, and  $1.0 \text{ mM}$   $\text{MnCl}_2$ . As described in the text, saturation of the rates is not achieved for every metal ion because phase II aggregation becomes evident at high concentrations of these metal ions. The data are not fit to a specific model. Solid lines are the "best smooth fit".

stacking. The relative rates of stacking in the presence of several concentrations of various metal ions are shown in Figure 5. In addition to the ions shown,  $\text{Fe}^{2+}$ ,  $\text{Ba}^{2+}$ , and  $\text{Ca}^{2+}$  were tested for their ability to support assembly of GS tubes. With addition of  $10 \text{ mM}$   $\text{Fe}^{2+}$ ,  $\text{Ba}^{2+}$ , or  $\text{Ca}^{2+}$  there is no detectable increase in scattered light intensity. The self-assembly reaction initiated by each metal ion was examined by EM. The stacked tubes obtained with  $\text{Cu}^{2+}$ ,  $\text{Cd}^{2+}$ ,  $\text{Ni}^{2+}$ , and  $\text{Hg}^{2+}$  appear structurally identical to those obtained with  $\text{Zn}^{2+}$  and  $\text{Co}^{2+}$  in EM micrographs (not shown). Presumably, the metal ions which support the stacking reaction all bind at the same site within GS. The relative potency of these metal ions in initiating formation of GS tubes at  $\text{pH } 7.0$ ,  $100 \text{ mM}$  KCl, and  $1 \text{ mM}$   $\text{MnCl}_2$  is  $\text{Cu}^{2+} > \text{Zn}^{2+}$ ,  $\text{Hg}^{2+} \gg \text{Cd}^{2+} > \text{Ni}^{2+}$ ,  $\text{Co}^{2+}$ . The concentration dependencies of the experimentally measured rate constants are summarized in Figure 5. Whereas  $\text{Cu}^{2+}$  provides a clear saturation point, at which the rate of stacking is not increased with additional metal, the other metal ions do not. This is because, as pointed out above, when the metal ion concentration is increased, phase II becomes evident in the kinetic traces before phase I is complete. Therefore, phase II contributes to the observed increase in light scattering intensity, and an accurate value for the rate constant cannot be determined. This suggests that metal ions may initiate phase II as well as phase I. This possibility will be examined in future studies. It is not known whether every metal binding site needs to be occupied in order for stacking to occur or whether every metal binding site accommodates a single metal ion.

## DISCUSSION

Glutamine synthetase from several bacterial sources has been shown previously to undergo supramolecular assembly to form fibers and higher order structures in the presence of  $\text{Zn}^{2+}$ ,  $\text{Mn}^{2+}$ , and  $\text{Co}^{2+}$  (Miller et al., 1974; Frey et al., 1975). Although these studies have examined collectively this reaction under different conditions, the previous experiments

have been done with GS preparations of varying purity and adenylation state. Thus, comparison of the results obtained in separate studies is difficult to interpret. Because this reaction exhibits properties that are desirable in the design of self-assembling nanostructures, we have initiated a systematic characterization of the *E. coli* GS assembly. During this characterization, we have discovered several important factors controlling the individual phases of GS supramolecular assembly. The assembly of GS dodecamers into high-order structures can be conveniently divided into two phases. We have quantitatively examined the first phase of this reaction, and we have qualitatively documented several factors which affect the second phase. This discussion will focus first on phase I and then on phase II.

Phase I consists of stacking of the individual dodecamers to form tubes or fibers. Obviously, the kinetics of this polymerization reaction are complex. Although it is possible that the rate of addition of GS dodecamers to the ends of a growing GS tube may be a function of tube length, as seen with assembly of thick filaments of myosin (Davis, 1993), no indication of positive or negative cooperativity in phase I of GS self-assembly has been documented. This is consistent with the observation that the lengths of tubes generated from GS stacking are not uniform, unlike assembled fibers of myosin (Davis, 1993). Assembled tubules of myosin are uniform in length due to negative cooperativity between tubule length and affinity of free myosin dimers for tubule ends.

Several factors affect the kinetics of the GS stacking reaction, including pH, salt concentration, and the identity of the metal ion. The kinetics of the  $\text{Zn}^{2+}$ - and  $\text{Co}^{2+}$ -mediated reactions have similar pH profiles, with a maximum at  $\text{pH } 7.25$ – $7.5$ . Given this pH dependence, it is tempting to speculate that histidine residues are required for the phase I reaction. This proposal is supported by the observation that pretreatment of GS samples with DEPC completely abolishes the  $\text{Zn}^{2+}$ -induced stacking behavior. Although we have not identified the specific histidine residues which are modified by DEPC, the intensity of the spectral change at  $230 \text{ nm}$  can be used to calculate the number of histidine residues which are modified. On the basis of this, it is apparent that modification of 2 histidines/subunit is sufficient to prohibit stacking. Examination of the crystal structure of the *S. typhimurium* GS reveals that 3 His residues are particularly exposed to solvent and would be expected to be susceptible to modification of DEPC. These are His-4, His-12, and His-387. The accompanying paper specifically addresses the role of His-4 and His-12 in this stacking reaction of *E. coli* GS. The observed pH dependence for phase I stacking is markedly different from the pH profile of the higher order aggregation reactions (phase II), as discussed below.

Phase I of the assembly reaction is also sensitive to the concentration of KCl or NaCl. Addition of  $10 \text{ mM}$  KCl is sufficient to slow the reaction by nearly 3-fold. This has significant implications for the molecular interactions involved. The decrease in the rate of the reaction accompanying an increase in ionic strength suggests that ionic interactions contribute to this aggregation. The fact that both KCl and NaCl are equally effective at inhibiting the stacking reaction suggests that there is not a specific monovalent cation binding site that alters the GS dodecameric structure to prevent stacking. Rather, the inhibition of the assembly

that is observed is likely due to a nonspecific, ionic strength effect. A similar dependence on KCl concentration was observed for the precipitation of GS from crude cell extracts (Miller et al., 1974).

One intriguing finding of these studies is that  $\text{Cu}^{2+}$  is more efficient than  $\text{Zn}^{2+}$  in mediating the stacking reaction. Furthermore,  $\text{Hg}^{2+}$  is nearly as potent as  $\text{Zn}^{2+}$ . It has been suggested previously that  $\text{Cu}^{2+}$  and  $\text{Hg}^{2+}$  ions are poor initiators of GS precipitation from crude cell extracts, relative to  $\text{Zn}^{2+}$  (Miller et al., 1974). It is possible that other  $\text{Hg}^{2+}$  binding and  $\text{Cu}^{2+}$  binding components in crude cell extracts diminish the apparent affinity for these ions. In particular,  $\text{Cu}^{2+}$  is expected to provide a useful spectroscopic probe for further characterization of the metal binding site responsible for this assembly reaction. Together with the relative affinities of the other metal ions that support GS stacking, these experiments should help to determine the molecular details of this metal binding site. It is striking that the metal ions which efficiently support this assembly reaction are all known to have some affinity for histidine-containing metal binding sites in other proteins (Karlin, 1993).

In addition to the effects of solution conditions on the rates of phase I stacking, these conditions markedly affect the side-to-side aggregation (phase II). Although we have not temporally isolated specific cable formation from nonspecific side-to-side association and cannot provide quantitative analysis of their susceptibility to solution conditions, several qualitative results are noteworthy. Perhaps the most striking observation regarding these higher order aggregation reactions is that they demonstrate a pH profile that is opposite phase I. Whereas the bimolecular rate constant for the phase I stacking reaction increases with pH, from pH 6.5–7.25, the side-to-side aggregation is fastest at acidic pHs. In fact, the phase II aggregation reaction may be partially inhibited by raising the pH to 7.5. This has significant implication for the commonly used  $\text{Zn}^{2+}$ -precipitation method of GS purification. Published protocols for this purification require acidification of crude preparations of GS to pH 5.8, before addition of  $\text{ZnCl}_2$ . Based on the results presented here, it is easy to rationalize the increased yield of GS protein when it is  $\text{Zn}^{2+}$ -precipitated at acidic pH from crude extracts. The efficient side-to-side aggregation of GS tubes leads to complete precipitation of paracrystalline aggregates, although they are presumably nonspecific, disordered complexes. Furthermore, the observation that phase II is apparently accelerated with increasing concentration of metal ions suggests that there is a specific metal binding site which mediates side-to-side interaction of the stacked tubules. The differential sensitivity of phase I and phase II aggregation to solution conditions provides a means for control of the structure of metal-dependent GS assemblies.

## ACKNOWLEDGMENT

The authors acknowledge Dr. Claudia Jochheim for helpful discussions and for preparation of figures.

## REFERENCES

- Almassy, R. J., Janson, C. A., Hamlin, R., Xuong, N. H., & Eisenberg, D. (1986) *Nature* 323, 304–309.
- Bhatia, S. K., Hickman, J. J., & Ligler, F. S. (1992) *J. Am. Chem. Soc.* 114, 4432–4433.
- Chen, Y. M., Backman, K., & Magasanik, B. (1982) *J. Bacteriol.* 150, 214–220.
- Colombo, G., & Villafranca, J. J. (1986) *J. Biol. Chem.* 261, 10587–10591.
- Dabrowski, M. J., Yanchunas, J., Jr., Villafranca, B. C., Dietze, E. C., Schurke, P., & Atkins, W. M. (1994) *Biochemistry* 33, 14957–14964.
- Davis, J. S. (1993) *Biochemistry* 32, 4035–4042.
- Denman, R. B., & Wedler, F. C. (1984) *Arch. Biochem. Biophys.* 232, 427–440.
- Frey, T. G., Eisenberg, D., & Eiserling, F. A. (1975) *Proc. Natl. Acad. Sci. U.S.A.* 72, 3402–3406.
- Frink, R. J., Eisenberg, D., & Glitz, D. G. (1978) *Proc. Natl. Acad. Sci. U.S.A.* 75, 5778–5782.
- Ghadiri, M. R., Soares, C., & Choi, C. (1992) *J. Am. Chem. Soc.* 114, 825–831.
- Ginsburg, A., Yeh, J., Hennig, S. B., & Denton, M. D. (1970) *Biochemistry* 9, 9633–9646.
- Gleiter, H. (1992) *Adv. Mater.* 4, 474–480.
- Grove, A., Mutter, M., Rivier, J. E., & Montal, M. (1993) *J. Am. Chem. Soc.* 115, 5919–5924.
- Heuer, A. H., Fink, D. J., Laraia, V. J., Arias, J. L., Calverty, P. D., Kendall, K., Wheeler, A. P., Veis, A., & Caplan, A. I. (1992) *Science* 255, 1098–1105.
- Jorgensen, W. L. (1993) *Proc. Natl. Acad. Sci. U.S.A.* 90, 1635–1636.
- Karlin, K. D. (1993) *Science* 261, 701–708.
- Liaw, S.-H., & Eisenberg, D. (1994) *Biochemistry* 33, 675–681.
- Liaw, S.-H., Pan, C., & Eisenberg, D. (1993) *Proc. Natl. Acad. Sci. U.S.A.* 90, 4996–5000.
- Maurizi, M. R., & Ginsburg, A. (1982) *J. Biol. Chem.* 257, 4271–4278.
- Maurizi, M. R., Kasprzyk, P. G., & Ginsburg, A. (1986) *Biochemistry* 25, 141–151.
- McGrath, K. P., Fournier, M. J., Mason, T. L., & Tirrel (1992) *J. Am. Chem. Soc.* 114, 727–733.
- Meldrum, F. C., Wade, V. J., Nimmo, D. L., Heywood, B. R., & Mann, S. (1991) *Nature* 349, 684–685.
- Merkler, D. J., Srikumar, K., Marchese-Ragone, S. P., & Wedler, F. C. (1988) *Biochim. Biophys. Acta* 952, 101–114.
- Miles, E. W. (1977) *Methods Enzymol.* 47, 431–443.
- Miller, R. E., Shelton, E., & Stadtman, E. R. (1974) *Arch. Biochem. Biophys.* 163, 155–171.
- O'Halloran, T. V. (1993) *Science* 261, 715–725.
- Ozin, G. A. (1992) *Adv. Mater.* 4, 612–649.
- Rowe, W. B., Ronzio, R. A., & Meister, A. (1969) *Biochemistry* 8, 2674–2679.
- Shrake, A. M., Fisher, M. T., McFarland, P. J., & Ginsburg (1989) *Biochemistry* 28, 6281–6290.
- Stadtman, E. R., Smyrniotis, P. Z., Davis, J. N., & Wittenberg, M. E. (1979) *Anal. Biochem.* 82, 275–281.
- Valentine, R. C., Shapiro, B. M., & Stadtman, E. R. (1968) *Biochemistry* 7, 2143–2152.
- Whitesides, G. M., Mathias, J. P., & Seto, C. T. (1992) *Science* 254, 1312–1319.
- Woolfolk, C. A., Shapiro, B. M., & Stadtman, E. R. (1966) *Arch. Biochem. Biophys.* 116, 171–192.
- Yamashita, M. M., Almassy, R. J., Janson, L. A., Lasek, D., & Eisenberg, D. (1989) *J. Biol. Chem.* 264, 17681–17689.